

Article

# CCAAT/Enhancer-Binding Protein Delta (C/EBP $\delta$ ): A Previously Unrecognized Tumor Suppressor that Limits the Oncogenic Potential of Pancreatic Ductal Adenocarcinoma Cells

Leonie Hartl <sup>1,2,\*,\dagger</sup>, JanWillem Duitman <sup>1,2,\dagger</sup>, Hella L. Aberson <sup>1</sup>, Kan Chen <sup>3</sup>, Frederike Dijk <sup>2,4</sup> , Joris J.T.H. Roelofs <sup>4</sup>, Mark P.G. Dings <sup>1,2</sup> , Gerrit K.J. Hooijer <sup>4</sup>, Pratika Y. Hernanda <sup>5</sup>, Qiunwei Pan <sup>3</sup>, Olivier R. Busch <sup>6</sup>, Marc G.H. Besselink <sup>7</sup>, Ton Boerman <sup>4</sup>, Maikel P. Peppelenbosch <sup>3</sup> , Maarten F. Bijlsma <sup>1,2,8,\ddagger</sup> and C. Arnold Spek <sup>1,2,\ddagger</sup> 

<sup>1</sup> Laboratory for Experimental Oncology and Radiobiology, Center for Experimental and Molecular Medicine, Amsterdam University Medical Center, University of Amsterdam, 1105 AZ Amsterdam, The Netherlands; j.w.duitman@amsterdamumc.nl (J.D.); h.l.aberson@amsterdamumc.nl (H.L.A.); m.p.dings@amsterdamumc.nl (M.P.G.D.); m.f.bijlsma@amsterdamumc.nl (M.F.B.); c.a.spek@amsterdamumc.nl (C.A.S.)

<sup>2</sup> Cancer Center Amsterdam, Amsterdam University Medical Center, University of Amsterdam, 1182 DB Amsterdam, The Netherlands; f.dijk@amc.uva.nl

<sup>3</sup> Department of Gastroenterology and Hepatology, Erasmus Medical Center, University Medical Center Rotterdam, 3015 GD Rotterdam, The Netherlands; chenkan@zstu.edu.cn (K.C.); q.pan@erasmusmc.nl (Q.P.); m.peppelenbosch@erasmusmc.nl (M.P.P.)

<sup>4</sup> Department of Pathology, Amsterdam University Medical Center, University of Amsterdam, 1105 AZ Amsterdam, The Netherlands; j.j.roelofs@amsterdamumc.nl (J.J.T.H.R.); g.k.hooijer@amsterdamumc.nl (G.K.J.H.); tonboerman@gmail.com (T.B.)

<sup>5</sup> Laboratory of Medical Genetics, University of Wijaya Kusuma Surabaya, Jawa Timur 60225, Indonesia; yuhyi\_h@uwks.ac.id

<sup>6</sup> Department of Surgery, Cancer Center Amsterdam, Amsterdam University Medical Center, University of Amsterdam, 1182 DB Amsterdam, The Netherlands; o.r.busch@amsterdamumc.nl

<sup>7</sup> Hepato-Pancreato-Biliary Surgery, Amsterdam University Medical Center, University of Amsterdam, 1105 AZ Amsterdam, The Netherlands; m.g.besselink@amsterdamumc.nl

<sup>8</sup> Oncode Institute, 3521 AL Utrecht Amsterdam, The Netherlands

\* Correspondence: l.hartl@amsterdamumc.nl; Tel.: +31-20-56-68-634

\dagger These authors contributed equally as first authors.

\ddagger These authors contributed equally as senior authors.

Received: 6 August 2020; Accepted: 3 September 2020; Published: 7 September 2020



**Simple Summary:** Here we show that a protein called C/EBP $\delta$  is present in healthy pancreas tissue but almost absent in pancreas tumors. Patients with less C/EBP $\delta$  in their tumors had the most metastases and the worst survival chances, showing that C/EBP $\delta$  has tumor-suppressive properties in pancreatic cancer. In this study, we reactivated C/EBP $\delta$  in pancreatic cancer cells *in vitro* and observed a reduction in cell proliferation in a 2-dimensional and 3-dimensional space. This implies that tumor cells grow slower when C/EBP $\delta$  is activated and they are likely also less capable to escape the primary tumor in order to form metastases. Conversely, when we deleted C/EBP $\delta$  in pancreatic cancer cells, we observed accelerated growth. We suggest that reactivating C/EBP $\delta$  can suppress tumor growth and formation of metastases, thereby improving patient survival.

**Abstract:** CCAAT/enhancer-binding protein  $\delta$  (C/EBP $\delta$ ) is a transcription factor involved in growth arrest and differentiation, which has consequently been suggested to harbor tumor suppressive activities. However, C/EBP $\delta$  over-expression correlates with poor prognosis in glioblastoma and promotes genomic instability in cervical cancer, hinting at an oncogenic role of C/EBP $\delta$  in these

contexts. Here, we explore the role of C/EBP $\delta$  in pancreatic cancer. We determined C/EBP $\delta$  expression in biopsies from pancreatic cancer patients using public gene-expression datasets and in-house tissue microarrays. We found that C/EBP $\delta$  is highly expressed in healthy pancreatic ductal cells but lost in pancreatic ductal adenocarcinoma. Furthermore, loss of C/EBP $\delta$  correlated with increased lymph node involvement and shorter overall survival in pancreatic ductal adenocarcinoma patients. In accordance with this, in vitro experiments showed reduced clonogenic capacity and proliferation of pancreatic ductal adenocarcinoma cells following C/EBP $\delta$  re-expression, concurrent with decreased sphere formation capacity in soft agar assays. We thus report a previously unrecognized but important tumor suppressor role of C/EBP $\delta$  in pancreatic ductal adenocarcinoma. This is of particular interest since only few tumor suppressors have been identified in the context of pancreatic cancer. Moreover, our findings suggest that restoration of C/EBP $\delta$  activity could hold therapeutic value in pancreatic ductal adenocarcinoma, although the latter claim needs to be substantiated in future studies.

**Keywords:** CCAAT/enhancer-binding protein delta; CEBPD; pancreatic ductal adenocarcinoma; PDAC; tumor suppressor; ampullary carcinoma; intrapancreatic cholangiocarcinoma

---

## 1. Introduction

Pancreatic cancer is a devastating disease with a survival outcome that is the worst of all human cancers [1]. The 5-year survival rate upon diagnosis is a little over 9% and overall mortality reaches 99% [2,3]. Due to the late onset of symptoms, only 15–20% of patients present with resectable disease, whereas the remaining patients present with metastatic or locally advanced disease, which cannot be resected. The median survival of the selected group of resectable patients, however, increases only to around 23 months whereas 5-year survival rates remain below 20% [4–6]. Eventually, the majority of these patients with a resectable primary tumor will succumb due to metastatic disease as well [7]. Thus, there is a clear clinical need to better understand the processes that drive pancreatic cancer and guide the development of novel avenues for rational treatment of this disease.

Ninety-five percent of pancreatic cancers arise from the exocrine compartment of the pancreas [8]. Of these exocrine tumors, pancreatic ductal adenocarcinoma comprises about 90% of all cases. In addition to pancreatic ductal adenocarcinoma, ampullary carcinoma and intrapancreatic cholangiocarcinoma may also be present within the pancreas due to their anatomical proximity, although these tumors are strictly taken as pancreatic cancers [9–11]. Ampullary carcinoma, with an incidence of around 0.6 cases in 100,000, arises in the ampulla of Vater, which is where the bile duct and pancreatic duct connect with the duodenum [9]. Intrapancreatic cholangiocarcinoma, with an incidence rate of 1–2 cases per 100,000, arises from epithelial cells of the bile duct (cholangiocytes) and is known as intrapancreatic bile duct cancer when it occurs where the bile duct passes through the pancreas [10,11]. The symptoms and pathology of intrapancreatic cholangiocarcinoma and pancreatic ductal adenocarcinoma are very similar and consequently these two types are difficult to distinguish.

Only a limited number of tumor suppressor genes have been formally established in pancreatic ductal adenocarcinoma. Mutations in genes such as *TP53*, *SMAD4*, *PTEN*, and *CDKN2A* are present in over 70% of pancreatic ductal adenocarcinomas, and mutations in these tumor suppressors are well known to drive tumor progression. As opposed to their clear biological relevance, mutations in tumor suppressor genes typically are of limited therapeutic value [12,13]. To improve patient treatment, the identification of tumor suppressor genes that could serve as therapeutic targets is therefore eagerly awaited.

CCAAT/enhancer-binding protein  $\delta$  (C/EBP $\delta$ ) is a member of the C/EBP superfamily of transcription factors, which consists of six unique members ( $\alpha$ ,  $\beta$ ,  $\gamma$ ,  $\delta$ ,  $\epsilon$  and  $\zeta$ ) [14]. Soon after its discovery, C/EBP $\delta$  was implied to act as a tumor suppressor by inducing growth arrest and differentiation in

breast cancer [15]. Indeed, C/EBP $\delta$  expression promotes CDC27 expression, leading to increased degradation of the cell cycle proteins cyclin D1, cyclin B1, Plk-1, and Skp2 [16]. Furthermore, expression of C/EBP $\delta$  is associated with downregulation of c-Myc and cyclin E, and upregulation of the cyclin-dependent kinase inhibitor p27 in the leukemia cell lines K562 and KCL22, leading to growth arrest and differentiation [17]. In A431 cervical cancer cells, C/EBP $\delta$  expression leads to the induction of apoptosis via the transcriptional regulation of the pro-apoptotic genes *PPARG2* and *GADD153* [18]. Moreover, C/EBP $\delta$  is involved in the regulation of pro-apoptotic gene expression and growth arrest during mammary gland involution [19,20]. In line with these data, C/EBP $\delta$  indeed acts as a tumor suppressor in breast cancer [21–23], ovarian serous carcinoma [24], cervical carcinoma [25], leukemia [26] and hepatocellular carcinoma [27,28].

In contrast to the presumed tumor suppressor role of C/EBP $\delta$ , several studies suggest that C/EBP $\delta$  may actually drive tumor progression in certain cancers. Indeed, C/EBP $\delta$  over-expression correlates with poor prognosis in glioblastoma [29]; it is required for efficient metastatic growth of mammary tumors [30], and drives proliferation and invasiveness of urothelial carcinoma cells, thereby driving metastatic disease leading to a reduced disease-specific survival [31]. Finally, C/EBP $\delta$  promotes tumorigenesis in the cervix by inducing aneuploidy and centromere abnormalities [32].

Taken together, the role of C/EBP $\delta$  in tumor biology seems more complex than originally anticipated and it does not seem to be a generic tumor suppressor. Instead, C/EBP $\delta$  may either suppress or promote tumor growth in a context specific manner. Here, we extend this notion by exploring the potential relevance of C/EBP $\delta$  in pancreatic cancer. We show that, despite its obvious importance for restraining cancer growth in a variety of systems, C/EBP $\delta$  takes on a tumor suppressive role in pancreatic ductal adenocarcinoma, while such effects remain insignificant, albeit not completely absent, in ampullary carcinoma or intrapancreatic cholangiocarcinoma. Moreover, we show that re-expressing C/EBP $\delta$  limits pancreatic cancer cell proliferation and future studies should elucidate whether it is of therapeutic interest in the treatment of this devastating disease.

## 2. Results

### 2.1. *CEBPD* mRNA Expression Is Decreased in Pancreatic Ductal Adenocarcinoma Tissue

To assess whether C/EBP $\delta$  may act as a tumor suppressor in pancreatic cancer, we first analyzed *CEBPD* mRNA expression levels in pancreatic ductal adenocarcinomas and in adjacent control tissue in publicly available gene expression datasets (GSE62452 [33] and GSE16515 [34]). As shown in Figure 1, *CEBPD* mRNA expression was observed in both tumor and non-tumor tissue in both datasets analyzed. Interestingly, however, *CEBPD* expression was decreased in tumor tissue as compared to the control tissue in both the GSE62452 (Figure 1A) and GSE16515 (Figure 1B) dataset. Subsequently, patients of the datasets were dichotomized into *CEBPD*-high and *CEBPD*-low groups whereupon differential gene expression analysis between these groups revealed enhanced expression of genes from published proliferation signatures [35,36] in patients of the *CEBPD*-low group opposed to the *CEBPD*-high group (data for GSE62452 shown in Figure 1C,D and Table S1). To corroborate these findings and provide statistics, we next performed gene set enrichment analyses of the proliferation signatures on the pancreatic cancer datasets. Samples were dichotomized by median *CEBPD* expression, and analysis showed a significant association with both signatures in the datasets (Figure 1E for the Ben-Porath proliferation gene set [35] and Figure 1F for the Chiang gene set [36], respectively, in GSE62452).

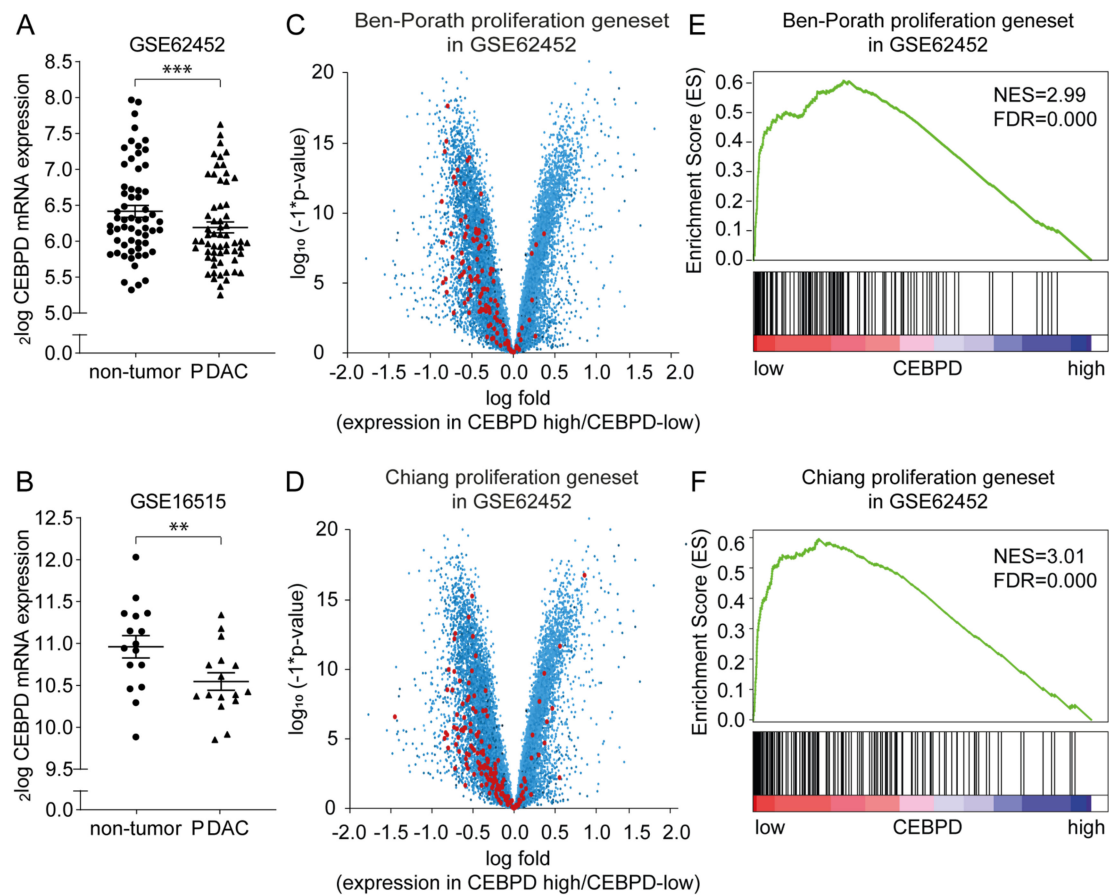


**Figure 1.** Analysis of publicly available datasets reveals *C/EBPδ* as a potential tumor suppressor in pancreatic ductal adenocarcinoma. (A,B) *CEBPD* gene expression in pancreatic ductal adenocarcinoma biopsies and adjacent healthy pancreatic tissue biopsies derived from GSE62452 (A) and GSE16515 (B). \*\*  $p < 0.01$ , \*\*\*  $p < 0.001$  compared to healthy control tissue. Lines indicate the mean  $\pm$  SEM. (C,D) Volcano plot of statistical significance against fold change between high and low *CEBPD* samples. Each data point represents a gene, while genes from the Ben-Porath [35] (C) or Chiang [36] (D) proliferation gene signatures are highlighted in red. Negative fold changes imply higher expression of a gene in the *CEBPD*-low group and vice versa. (E,F) Gene set enrichment analysis (GSEA) using the Ben-Porath (E) or Chiang (F) proliferation gene signatures on patients with high or low *CEBPD* expression levels in GSE62452. GSEA: gene set enrichment analysis, NES: normalized enrichment score, FDR: false discovery rate.

## 2.2. *C/EBPδ* Protein Levels Are Decreased in Pancreatic Ductal Adenocarcinoma but Not in Ampullary Carcinoma or Intrapancreatic Cholangiocarcinoma

*C/EBPδ* is a ubiquitously expressed transcription factor which is not specific to epithelial (tumor) cells but also expressed in cell types of the stromal compartment including pancreatic stellate cells [37]. Indeed, *CEBPD* expression levels correlate with stromal gene signatures in five out of six publicly available datasets containing pancreatic ductal adenocarcinoma (PDAC) samples [34,38–42] as determined using ESTIMATE [43] (Table S2 and Figure S1). Moreover, for transcriptional activity of *C/EBPδ*, only nuclear expression is relevant and gene expression levels of tissue biopsies such as those used in the bioinformatics experiments described above may consequently not accurately reflect the *C/EBPδ* activity that is relevant for tumor cell biology. To circumvent these confounding effects of whole biopsy gene expression analysis, we subsequently immunohistochemically analyzed nuclear *C/EBPδ* protein levels in tumor cells of a cohort of 67 pancreatic ductal adenocarcinoma patients using normal duct epithelium as control. *C/EBPδ* was highly expressed in normal, non-tumorigenic,

pancreatic ductal cells (Figure 2A,B). The vast majority of normal pancreatic ductal cells showed strong nuclear C/EBP $\delta$  staining. Interestingly, C/EBP $\delta$  expression was significantly decreased in pancreatic ductal adenocarcinoma cells (Figure 2C–G). Although some cytoplasmic staining was still observed in pancreatic ductal adenocarcinoma biopsies, most of the tumor cell nuclei were negative for C/EBP $\delta$  or the intensity was very much decreased compared to normal tissue.

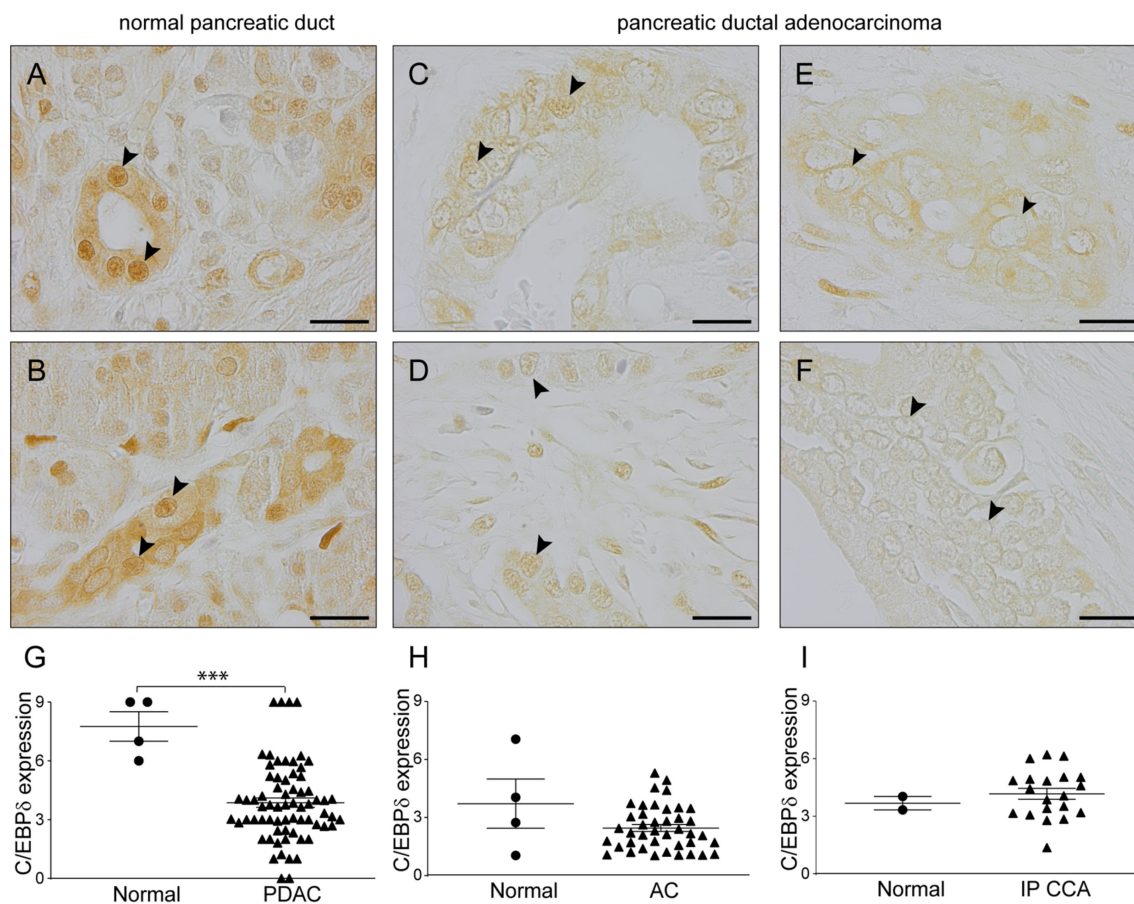


**Figure 2.** C/EBP $\delta$  expression is decreased in the nuclei of pancreatic ductal adenocarcinoma cells. Immunohistochemical staining of C/EBP $\delta$  shows strong expression in healthy pancreatic tissue (A,B) and decreased (C,D) or no expression (E,F) in pancreatic ductal adenocarcinoma. Representative tumor nuclei are indicated with black arrowheads. Quantification of nuclear C/EBP $\delta$  expression levels in healthy control tissue (G–I), pancreatic ductal adenocarcinoma (G), ampullary carcinoma (H) and intrapancreatic cholangiocarcinoma (I). \*\*\*  $p < 0.001$  compared to healthy control tissue. Lines indicate the mean  $\pm$  SEM. PDAC: pancreatic ductal adenocarcinoma, AC: ampullary carcinoma, IP CCA: intrapancreatic cholangiocarcinoma. Scale bars: 20  $\mu$ m.

To determine whether the observed decrease in nuclear C/EBP $\delta$  expression in pancreatic cancer is specific to pancreatic ductal adenocarcinomas or whether it is a more general phenomenon, we also determined nuclear C/EBP $\delta$  expression levels in ampullary carcinoma and intrapancreatic cholangiocarcinoma. We found that C/EBP $\delta$  expression levels were relatively low in the nuclei of normal intestinal epithelial cells within the ampulla of Vater (Figure 2H) and in normal cholangiocytes (Figure 2I) compared to normal pancreatic ductal cells. Moreover, nuclear C/EBP $\delta$  expression was not further decreased in tumor cells of these cancer types and semi-quantitative analysis of C/EBP $\delta$  expression levels showed no significant difference between normal and tumor cell nuclei in these patients (Figure 2H,I).

### 2.3. C/EBP $\delta$ Protein Expression Is Associated with Regional Lymph Node Involvement and Correlates with Overall Survival in Pancreatic Ductal Adenocarcinoma

To assess the potential clinical relevance of reduced C/EBP $\delta$  expression in pancreatic ductal adenocarcinoma, we first determined whether C/EBP $\delta$  correlated with lymph node involvement in these patients. As shown in Figure 3A and Table 1, C/EBP $\delta$  expression in the nuclei of primary tumors was significantly decreased in patients with tumor cell positive regional lymph nodes (N1) compared to patients without tumor cell positive regional lymph nodes (N0). This association of C/EBP $\delta$  protein levels with N-status was absent in ampullary carcinoma (Figure 3B) and intrapancreatic cholangiocarcinoma (Figure 3C). In line with metastasis to local lymph nodes, decreased nuclear C/EBP $\delta$  expression was also significantly correlated with shorter overall survival in pancreatic ductal adenocarcinoma patients (Figure 3D). Median survival of pancreatic ductal adenocarcinoma patients in the lower half of C/EBP $\delta$  expression was 16.9 months, whereas median survival of patients in the upper half of C/EBP $\delta$  expression was 22.2 months ( $p < 0.05$ ). Compared to pancreatic ductal adenocarcinoma, patients with ampullary carcinoma (Figure 3E) or intrapancreatic cholangiocarcinoma (Figure 3F) showed a longer median overall survival of 49.9 and 24.4 months, respectively (versus 18.3 months for the pancreatic ductal adenocarcinoma patients). As expected based on similar C/EBP $\delta$  expression and the lack of association with regional lymph node involvement, C/EBP $\delta$  expression also did not correlate significantly with overall survival in ampullary carcinoma and intrapancreatic cholangiocarcinoma. These results lead to the notion that C/EBP $\delta$  may act as a tumor suppressor in pancreatic ductal adenocarcinoma, while this relation is not observed in ampullary carcinoma or intrapancreatic cholangiocarcinoma.

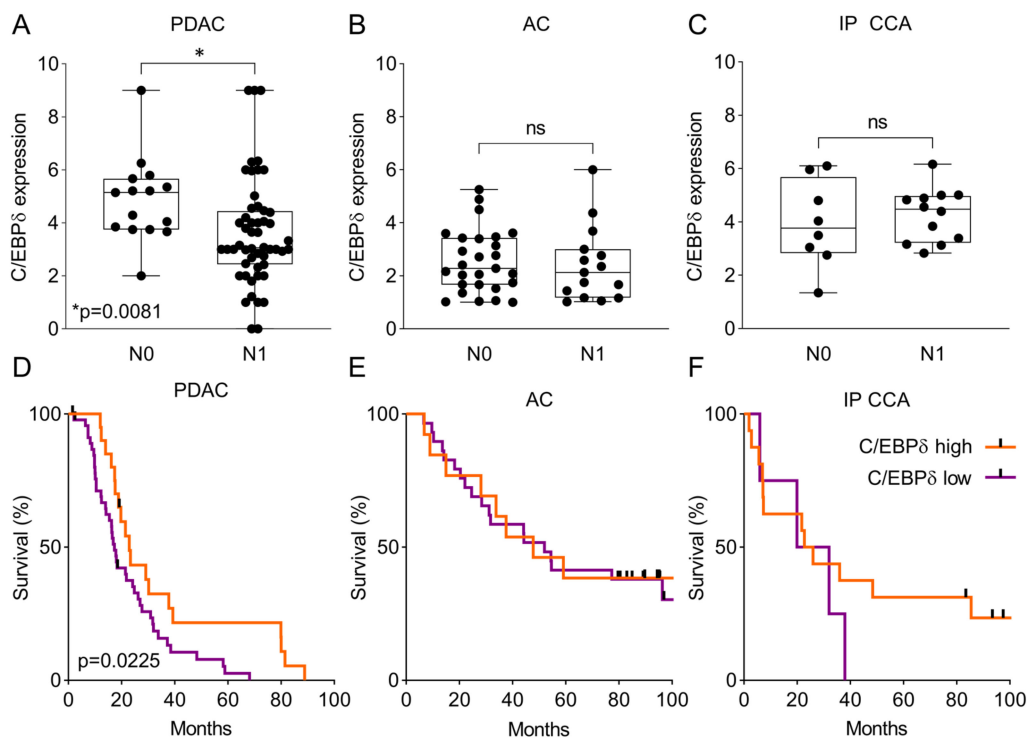


**Figure 3.** C/EBP $\delta$  expression correlates with regional lymph node metastasis and overall survival in pancreatic ductal adenocarcinoma patients. (A–C) C/EBP $\delta$  expression levels in patients with and without regional lymph node metastasis (N0: negative regional lymph nodes, N1: positive regional lymph nodes) in pancreatic ductal adenocarcinoma (A), ampullary carcinoma (B) and intrapancreatic cholangiocarcinoma (C). (D–F) Overall survival in pancreatic ductal adenocarcinoma (D), ampullary carcinoma (E) and intrapancreatic cholangiocarcinoma (F) in different groups of C/EBP $\delta$  expression levels. Vertical black bars in Kaplan-Meier plots represent censored patients. ns: not significant.

**Table 1.** N-status correlates to C/EBP $\delta$  protein expression in pancreatic ductal adenocarcinoma patients.

N-Status	C/EBP $\delta$ Expression	
	Low	High
	(N = 47)	(N = 20)
N0	7	8
N1	40	12
Fisher's exact test	$p = 0.029$	
Median survival (months)	16.9	22.2

#### 2.4. C/EBP $\delta$ Modulates Oncogenesis of Pancreatic Ductal Adenocarcinoma Cells

##### 2.4.1. C/EBP $\delta$ Over-Expression Reduces Proliferation of Pancreatic Ductal Adenocarcinoma Cells

To further validate the potential tumor-suppressive effects of C/EBP $\delta$  in pancreatic ductal adenocarcinoma, we conducted in vitro clonogenic assays with two commonly used pancreatic ductal adenocarcinoma cell lines, PANC-1 and MIA PaCa-2. From publicly available mRNA expression datasets, we know that both these cell lines show low baseline expression levels of *CEBPD* which is in line with the low expression levels observed in pancreatic ductal adenocarcinoma patients, making them a solid model for C/EBP $\delta$  over-expression studies. First, we assessed the effect of transient C/EBP $\delta$  over-expression on the clonogenic capacity of PANC-1 cells. To this end, 100 control- or *CEBPD*-transfected cells were seeded into 24-well plates after which colony formation was observed over time. As shown in Figure 4A, we observed a significant reduction in clonal outgrowth by C/EBP $\delta$  over-expressing cells as compared to control cells ( $p < 0.005$ ). To corroborate these findings, we next seeded single control- or *CEBPD*-transfected cells in 96-well plates. Similar to the 100 cells per well approach, *CEBPD* over-expression decreased the clonogenic capacity of PANC-1 cells. Indeed, *CEBPD*-over-expressing cells showed a clonogenic capacity of 8% ( $N = 23$  colonies out of 288 single cells) as compared to 16% in control-transfected cells ( $N = 46$  colonies out of 288 single cells), constituting a decrease of 50% in clonogenic capacity ( $\chi^2$  test,  $p = 0.0032$ ).

As C/EBP $\delta$  is expected to dilute out in transient transfection experiments, we next performed stable transfection experiments. To this end, PANC-1 and MIA PaCa-2 cells were transduced with a *CEBPD*-IRES-EGFP over-expression plasmid; after which, cells were sorted into three fractions based on eGFP fluorescence (Figure 4B). Importantly, both C/EBP $\delta$  and eGFP were indeed over-expressed in transduced cells (Figure 4C) and *CEBPD* expression correlated with EGFP expression (Figure 4D). Subsequent clonogenic experiments with 500 transduced cells of each fraction seeded in 12-well plates confirmed the transient transfection experiments by showing that C/EBP $\delta$  expression was negatively correlated with colony formation in both cell lines (PANC-1 low expression: 114 colonies; intermediate expression: 83 colonies; high expression: 52 colonies. MIA PaCa-2 low expression: 75 colonies; intermediate expression: 56 colonies; high expression: 41 colonies) (Figure 4E,F). Altogether, these in vitro experiments imply that C/EBP $\delta$  indeed limits the growth of pancreatic ductal adenocarcinoma cells.

##### 2.4.2. A Tet-on System Reveals Dose-Dependent Effects of C/EBP $\delta$ on Proliferation and Clonogenicity

To widen our understanding of the effects of C/EBP $\delta$  on pancreatic adenocarcinoma cells, we turned to a doxycycline-inducible Tet-On system. As shown in Figure 5A–F, this system permits tightly controlled expression of C/EBP $\delta$  with induction levels at the 2000 ng/mL doxycycline dose, mimicking the fold-change in protein expression observed in tumor versus normal patient samples. As observed with constitutive over-expression, controlled over-expression of C/EBP $\delta$  curbed proliferation of pancreatic adenocarcinoma cells. Interestingly, subjecting the cells to a concentration of 100 ng/mL doxycycline, which minimally induces C/EBP $\delta$ , already moderately reduced proliferation of PANC-1

while a concentration of 2000 ng/mL significantly reduced proliferation in both PANC-1 and MIA PaCa-2 (Figure 5G,H).

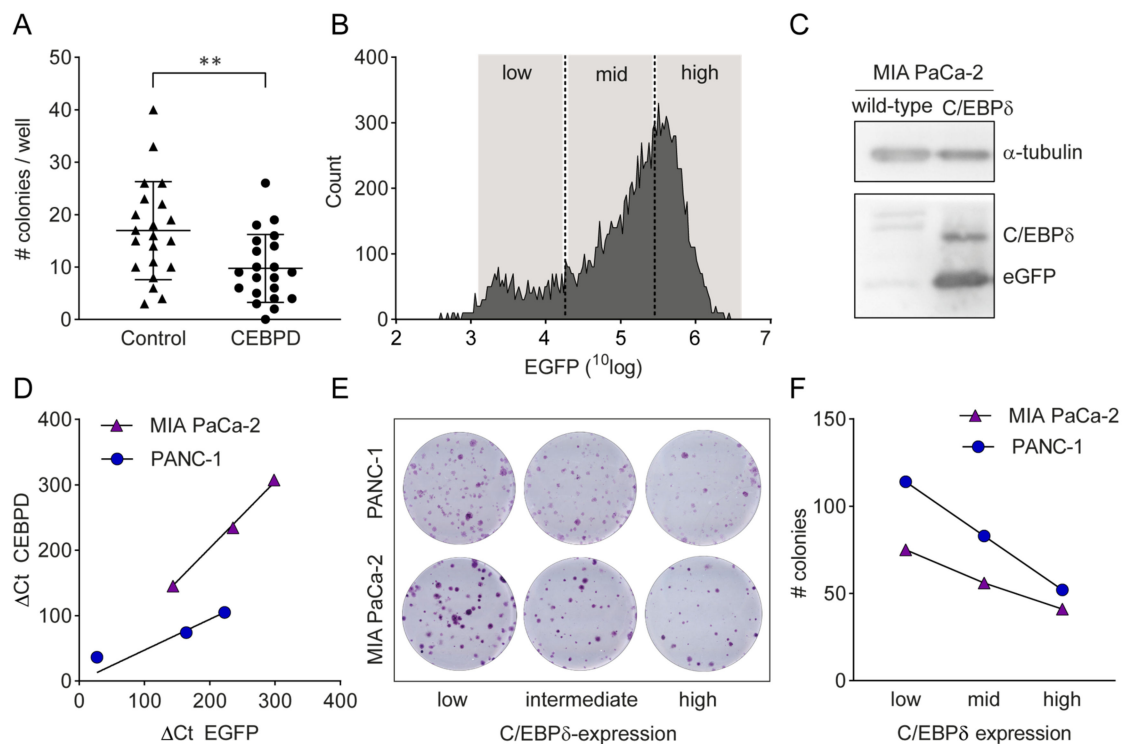


**Figure 4.** C/EBPδ over-expression inhibits clonogenicity in PANC-1 and MIA PaCa-2 cells. (A) Average number of colonies grown out from 100 C/EBPδ-over-expressing or control-transfected PANC-1 cells per well in three independent experiments ( $N = 21$ ). Lines indicate the mean  $\pm$  SEM. \*\*  $p < 0.005$ . Out of 2100 control-transfected cells, 356 grew into a colony. Only 205 out of 2100 C/EBPδ over-expressing cells grew out a colony. (B) Histogram and gating of CEBPD-IRES-EGFP-transduced MIA PaCa-2 cells. (C) Western blot showing over-expression of C/EBPδ and eGFP protein after transfection. The uncropped blots are provided in Figure S2. (D) CEBPD and EGFP mRNA expression of CEBPD-IRES-EGFP-transduced cells sorted by EGFP-fluorescence. Quantitative RT-PCR confirmed elevated CEBPD mRNA expression in cells expressing high EGFP mRNA (MIA PaCa-2:  $R^2 = 0.9975$ , \*  $p < 0.05$ ; PANC-1:  $R^2 = 0.9724$ ,  $p = 0.0531$ ). (E) Clonogenic assay of PANC-1 and MIA PaCa-2 cells expressing C/EBPδ at varying levels. (F) C/EBPδ expression correlates with colony formation efficiency. Plotting the number of colonies from Figure 4E against the respective CEBPD mRNA expression shows a dependency of colony formation efficiency on CEBPD levels in PANC-1 and MIA PaCa-2 cells.

Next, we assessed the limiting effects of C/EBPδ on colony formation of pancreatic adenocarcinoma cells. Seeding single cells in 96-well plates, we found that 2000 ng/mL doxycycline reduced single cell outgrowth by 32% in MIA PaCa-2 and by 12% in PANC-1 cells (data not shown). The observed reduction in clonogenicity was lower compared to that seen in the constitutive system shown in Figure 4 which is well in accordance with the difference in C/EBPδ expression between the two systems and again emphasizes that these effects are dose-dependent on C/EBPδ.

In addition to two-dimensional clonogenic and proliferation assays, we next assessed anchorage-independent growth in three-dimensional soft agar sphere formation assays. This assay constitutes a well-recognized measure of stemness and malignant potential owed to anchorage-independent out-growth of a single cell [44]. As in two-dimensional clonogenic assays, we also observed a decrease in tumor sphere formation when comparing doxycycline-treated C/EBPδ over-expressing cells to untreated low C/EBPδ expressing cells. Interestingly, 100 ng/mL doxycycline already significantly limited sphere formation in PANC-1 cells but had no effect in MIA PaCa-2 cells.

The 2000 ng/mL doxycycline dose again drastically suppressed sphere formation by PANC-1 and also, to some extent, reduced the number of spheres formed by MIA PaCa-2 cells although this difference did not reach significance (Figure 5I,J).

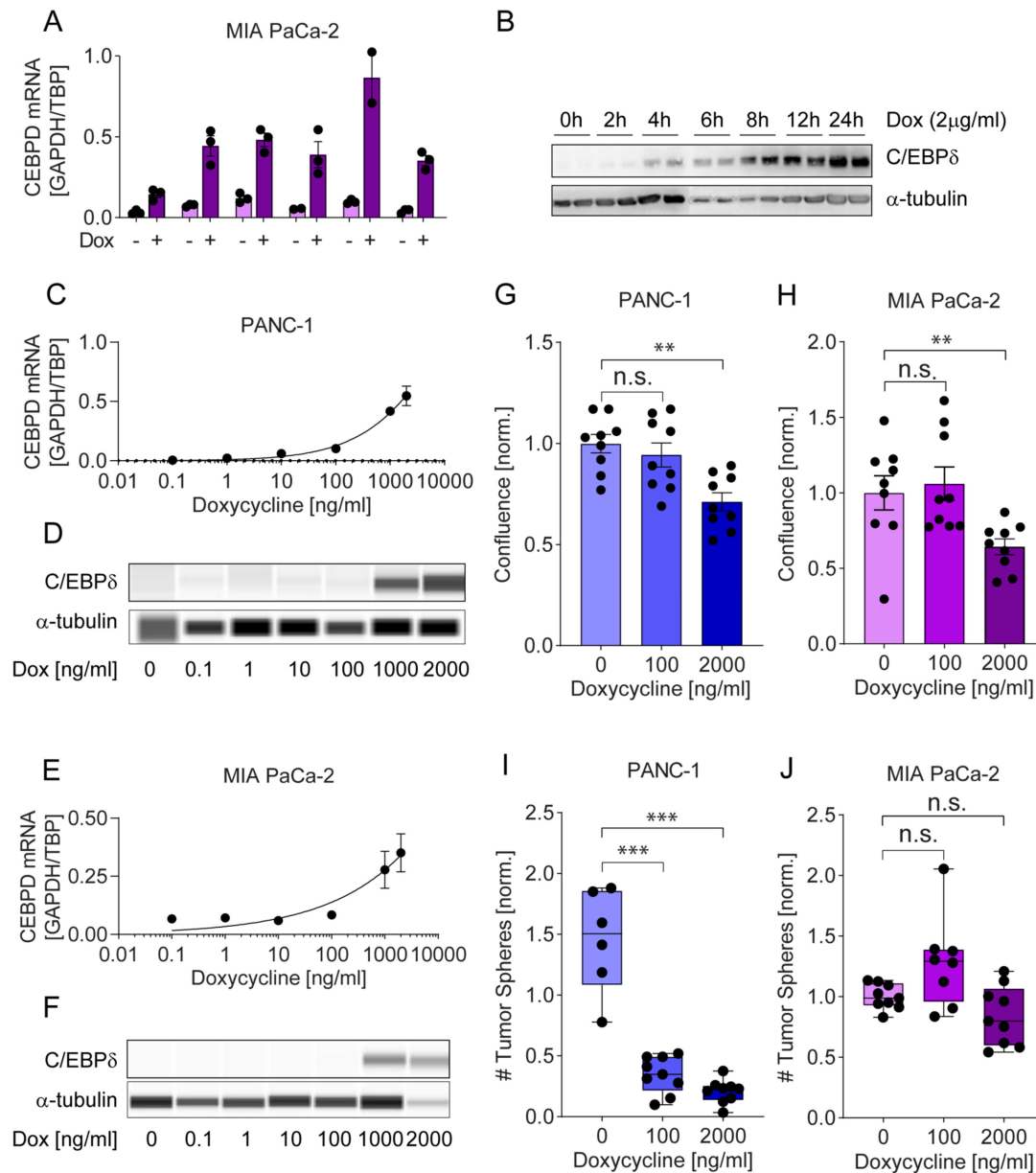


**Figure 5.** Doxycycline dose-dependent induction of C/EBPδ regulates proliferation and tumor sphere formation. (A) Single clones of MIA PaCa-2 cells, transduced with a doxycycline-inducible C/EBPδ over-expression plasmid, show increased C/EBPδ mRNA levels upon induction. (B) C/EBPδ induction in MIA PaCa-2 cells over time. The uncropped blots are provided in Figure S3A (C–F) Doxycycline dose-dependently induces C/EBPδ in both transduced MIA PaCa-2 and PANC-1 cells. The uncropped blots are provided in Figure S3B,C. (G,H) Proliferation is mildly decreased by 100 ng/mL and significantly reduced by 2000 ng/mL doxycycline in PANC-1 (\*\*  $p = 0.0012$ ) and MIA PaCa-2 (\*\*  $p = 0.0078$ ) cells. (I,J) Tumor sphere formation in soft agar is significantly reduced by 100 and 2000 ng/mL doxycycline in PANC-2 (\*\*\*  $p = 0.0004$ ). A similar yet not significant trend is observed in MIA PaCa-2 with 2000 ng/mL doxycycline. Dox: Doxycycline. n.s.: not significant, \*\*\*  $p < 0.001$ .

### 2.4.3. Silencing C/EBP $\delta$ Enhances Proliferation of Pancreatic Ductal Adenocarcinoma Cells

Considering the finding that over-expressing C/EBP $\delta$  reduces the proliferation of pancreatic ductal adenocarcinoma cells, thereby decreasing their malignant potential, we next asked whether silencing C/EBP $\delta$  would conversely trigger proliferation. As both PANC-1 and Mia PaCa-2 cells already express very low or undetectable C/EBP $\delta$  levels, we turned to Capan-2 cells that, according to public gene expression datasets, show the highest *CEBPD* levels of all routinely used pancreatic cancer cell lines (Figure S4) [45,46]. Interestingly, shRNA *CEBPD*-silenced Capan-2 cells (silencing efficiency in Figure 6A) indeed showed increased proliferation rates as compared to control-silenced cells (Figure 6B). Notably, more efficient silencing corresponded to progressively increased proliferative capabilities, underscoring the dose-dependent effect of C/EBP $\delta$  on pancreatic adenocarcinoma cell behavior.

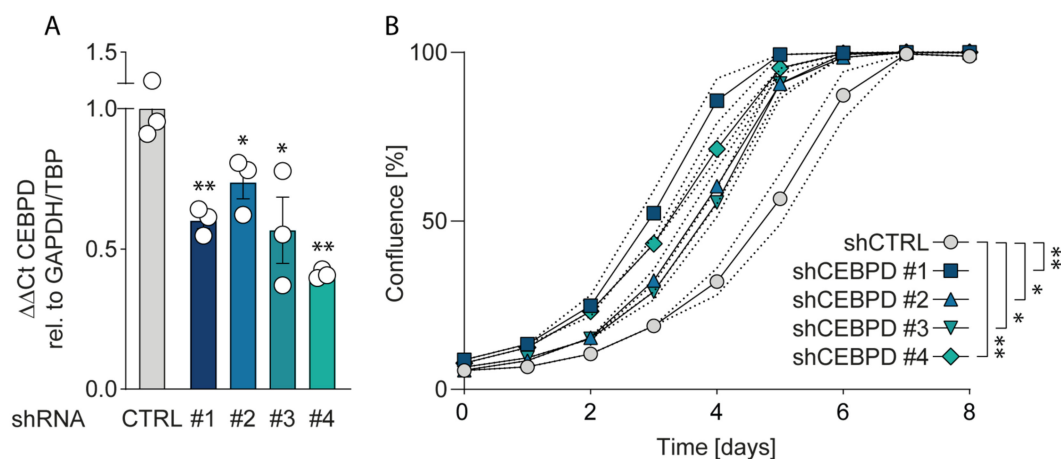


**Figure 6.** Silencing C/EBP $\delta$  enhances proliferation of Capan-2 cells. **(A)** Quantitative RT-PCR shows decreased levels of *CEBPD* mRNA in Capan-2 cells stably expressing shRNAs against *CEBPD*. ( $p = **0.0058$ ,  $*0.0429$ ,  $*0.0338$  and  $**0.001$  for shCTRL vs. shCEBPD #1, #2, #2 and #4, respectively). **(B)** Proliferation of *CEBPD*-silenced Capan-2 cells is significantly increased compared to control cells. ( $p = **0.0013$ ,  $*0.011$ ,  $*0.0146$  and  $**0.0013$  for shCTRL vs. shCEBPD #1, #2, #2 and #4, respectively).

### 3. Discussion

C/EBP $\delta$  has been found to negatively affect tumor growth by inducing growth arrest and differentiation [21–28]. Recently, however, C/EBP $\delta$  was also suggested to drive tumor progression and/or metastasis in certain tumor types [29–32], suggesting that C/EBP $\delta$  may either suppress or promote tumor progression in a context specific manner. Here, we explore the importance of C/EBP $\delta$  in pancreatic cancer and show that C/EBP $\delta$  harbors tumor suppressor activity in pancreatic ductal adenocarcinoma and that re-expressing C/EBP $\delta$  in pancreatic adenocarcinoma cells curbs clonogenicity and proliferation.

Data mining of publicly available microarray datasets showed that *CEBPD* gene expression is significantly decreased in pancreatic ductal adenocarcinomas versus healthy pancreatic tissue. Although of obvious interest, whole tumor biopsy *CEBPD* expression levels do not necessarily correspond to C/EBP $\delta$  activity in tumor cells. In addition to confounding expression of *CEBPD* in stromal cells, expression levels in whole tumor biopsies may also not fully represent nuclear C/EBP $\delta$  activity. Subsequent immunohistochemical analyses of tissue arrays underscore this notion and indeed show both stromal and cytoplasmic staining. Of interest, in pancreatic tissue biopsies, healthy ductal cells express high nuclear levels of C/EBP $\delta$  which is at odds with the general notion that C/EBP $\delta$  expression is typically low under normal conditions [47]. More importantly, C/EBP $\delta$  levels are dramatically reduced in ductal adenocarcinoma cells as compared to normal ductal cells. As C/EBP $\delta$  induces growth arrest [16,17], it is tempting to speculate that the loss of C/EBP $\delta$  conversely facilitates

tumorigenesis. Such a role of C/EBP $\delta$  would be in line with previous studies showing that C/EBP $\delta$  is a tumor suppressor in leukemia, breast cancer, hepatocellular carcinoma and cervical cancer [21–28].

We were able to confirm that C/EBP $\delta$  expression is low in MIA PaCa-2 and PANC-1, two commonly used pancreatic ductal adenocarcinoma cell lines. This is in line with our observations in pancreatic cancer patients and with a potential role of C/EBP $\delta$  as a tumor suppressor in pancreatic cancer. More importantly, their low C/EBP $\delta$  expression makes these cells suitable model systems for C/EBP $\delta$  re-expression studies with the assumption that rescuing C/EBP $\delta$  expression would reduce their tumorigenic capacity in case C/EBP $\delta$  acts as a genuine tumor suppressor. PANC-1 and MIA PaCa-2 cells indeed showed decreased proliferation and clonogenicity upon C/EBP $\delta$  re-expression. Additionally, these effects were dose dependent, implying a relation between tumorigenicity and C/EBP $\delta$  expression levels. Conversely, shRNA-dependent silencing of C/EBP $\delta$  enhances proliferation in a dose-dependent manner strongly suggesting that C/EBP $\delta$  expression levels negatively correlate with the proliferative capacity of pancreatic ductal adenocarcinoma cells.

Next to driving proliferation and clonogenicity of pancreatic ductal adenocarcinoma cells, loss of C/EBP $\delta$  also seems to promote anchorage-independent growth. This clonogenic capacity in a three-dimensional, anchorage-free environment is considered a key hallmark of oncogenic transformation and is considered the most accurate and stringent in vitro assay for detecting malignant transformation of cells. We found a marked reduction in the number of spheres formed by two pancreatic adenocarcinoma cell lines upon re-expression of C/EBP $\delta$ . Interestingly, although C/EBP $\delta$  re-expression limits sphere formation in both PANC-1 and MIA PaCa-2 cells, PANC-1 cells appear to be more susceptible to reversing oncogenic properties upon C/EBP $\delta$  induction. Although the precise mechanism underlying the reduction in anchorage-independent growth of pancreatic adenocarcinoma cancer cell remains to be established, it is tempting to speculate that these data explain the correlation found between C/EBP $\delta$  expression and lymph node invasion observed in our patient cohort. Indeed, anchorage-independent growth is strongly associated with the metastatic potential of cancer cells [44]. Irrespective of the actual mechanism, the reduced overall survival in pancreatic ductal adenocarcinoma patients with low C/EBP $\delta$  levels might be directly linked to the increased lymph node metastases in these patients.

Taken together, our results point towards a clear direction where C/EBP $\delta$  regulates the proliferation and clonogenic capacities of PDAC cells. However, as two-dimensional monoculture experiments in vitro cannot account for important factors, such as stromal and immune infiltration, in vivo validation of these findings is urgently needed to manifest the notion that C/EBP $\delta$  might act as a tumor suppressor in PDAC.

C/EBP $\delta$  is obviously not the first tumor suppressor identified in pancreatic adenocarcinoma. Indeed, genes such as *TP53*, *SMAD4*, *PTEN*, and *CDKN2A* are well-known tumor suppressors and mutations in these genes, which are present in over 70% of pancreatic ductal adenocarcinomas, drive tumor progression. As opposed to the other classical tumor suppressors, C/EBP $\delta$  seems, however, neither hypermethylated, nor mutated, lost or deleted in pancreatic adenocarcinoma (re-analysis of previously published data [48–50]) suggesting re-activation of C/EBP $\delta$  may hold therapeutic promise in the setting of pancreatic adenocarcinoma. Although C/EBP $\delta$  re-expression indeed limits proliferation and clonogenicity in pancreatic adenocarcinoma cell lines, future studies should prove or refute this hypothesis.

The mechanism via which C/EBP $\delta$  exerts its tumor suppressive and anti-metastatic effects remains elusive. In an attempt to uncover the underlying mechanism, we have investigated the expression of different putative targets of C/EBP $\delta$  involved in cell cycle progression, apoptosis, stemness and the leading-edge genes of the above described gene set enrichment analyses (GSEAs) (Figure S5). Enhanced expression of *CDKN1A* (p21) along with suppressed cyclin-dependent kinases *CDK1*, *CDK2* and *CDK6* point towards cell cycle arrest as a main mechanism of the observed C/EBP $\delta$ -induced effects in PDAC cells. Interestingly, however, C/EBP $\delta$  also appears to affect almost all of the other investigated pathways to some degree. Hence, the data are not as straightforward as expected and do

not allow firm conclusions on the downstream pathways affected by C/EBP $\delta$ . High-throughput RNAseq experiments will be deployed to uncover the major driving mechanism underlying C/EBP $\delta$ 's role in PDAC. These will be valuable in the view of molecular biology as well as for the discovery of new clinical targets in the treatment of PDAC.

To date, several agents have been described to effectively induce C/EBP $\delta$  expression. Among these activators are interleukin-6, which elicited growth-inhibiting effects on LNCaP prostate cancer cells via C/EBP $\delta$  activation [51], 1-(2-hydroxy-5-methylphenyl)-3-phenyl-1, 3-propanedione (HMDB), which attenuated the growth of A431 epidermoid carcinoma xenografts in severe combined immunodeficient mice [18,27], and metformin, which induced autophagy of Huh7 liver cancer cells via C/EBP $\delta$  activation [52]. Next to that, C/EBP $\delta$  has been induced by various external stimuli in the inflammatory context [53]. Preliminary experiments did not show a significant effect of any of these compounds on CEBPD expression in pancreatic adenocarcinoma cells and further studies are needed to find potent upstream regulators of C/EBP  $\delta$  in this context.

In contrast to our observation that the loss of C/EBP $\delta$  is associated with increased lymph node metastasis and subsequent poor prognosis, it has recently been shown that C/EBP $\delta$  amplification drives tumor metastasis in urothelial carcinoma [31]. These latter data are in line with a study showing that C/EBP $\delta$  over-expression correlates with poor prognosis in glioblastoma [29]. A picture thus emerges that C/EBP $\delta$  may act either as a tumor suppressor or as an oncogene in a context-dependent manner. In line with this notion, we show here that C/EBP $\delta$  levels in two other tumors that are located within the pancreas, i.e., ampullary carcinoma and intrapancreatic cholangiocarcinoma, do not differ significantly from control levels in normal intestinal epithelial cells and cholangiocytes, respectively. More importantly, we could not identify a correlation of either patient survival or lymph node status with C/EBP $\delta$  expression in ampullary carcinoma or intrapancreatic cholangiocarcinoma patients based on which we propose that C/EBP $\delta$  is unlikely to act as a tumor suppressor in these cancers. Although it may be tempting to suggest that the baseline expression of C/EBP $\delta$  in healthy tissues can generally determine the sensitivity of an arising tumor to the tumor suppressive effects of C/EBP $\delta$ , the questions of what determines whether C/EBP $\delta$  acts as tumor promotor or tumor suppressor remains to be answered.

## 4. Materials and Methods

### 4.1. Mining of Publicly Available RNA Microarray Datasets

Datasets were derived from Gene Expression Omnibus [48] using the R2 microarray analysis and visualization platform [46]. CEBPD expression levels were derived from two different datasets, i.e., GSE62452 (updated version of GSE28735 [33] with an extra 16 tumor and control biopsies) and GSE16515 [34]. From the GSE16515 dataset, we only included patients of which paired tumor and adjacent non-tumor biopsies were available. Gene set enrichment analysis (GSEA) was performed using the Broad Institute tool [49]. Samples were dichotomized by median CEBPD expression. *p*-values indicating the significance of enrichment were determined by 1000 permutations using the Ben-Porath [35] and Chiang [36] proliferation gene sets.

### 4.2. Tissue Microarray (TMA)

Formalin-fixed, paraffin-embedded biopsies from 129 pancreatic cancer cases between the years of 1983 and 2015 were used for compilation of tissue microarrays (TMAs) using routine procedures. Biopsies were selected from the archives of the Pathology Department at the Amsterdam University Medical Center, Amsterdam. The study was approved by the investigator's institutional review boards. Patients with a known previous malignancy in another organ were excluded from the analysis. The current study included 89 men (69.8%) and 40 women (30.2%), their ages range from 47 to 83 years, with a mean ( $\pm$ SD) of 64.4 ( $\pm$ 8.9) and median of 65 years (Table 2). Sixty-seven patients were diagnosed with pancreatic ductal adenocarcinoma, 42 with ampullary carcinoma and 20 with intrapancreatic cholangiocarcinoma. For 104 of the patients, 3 cores were available each (43 pancreatic

ductal adenocarcinoma, 20 intrapancreatic cholangiocarcinoma, 41 ampullary carcinoma). Each core received an individual score as described in 4.4. For 25 patients, only one core was available (24 pancreatic ductal adenocarcinoma, 1 ampullary carcinoma). From each of these cores, three tumor-cell containing locations were selected at random and nuclear C/EBP $\delta$  staining was quantified as described in 4.4. Six biopsies of normal pancreas tissue were included to serve as healthy control and C/EBP $\delta$  staining was quantified as described in 4.4.

**Table 2.** Characteristics of patients included in the cohort.

Characteristic	PDAC (N = 67)		AC (N = 42)		IP CCA (N = 20)	
	N	%	N	%	N	%
Median age (range) (years)	63 (47–83)		66.5 (48–78)		64.5 (49–82)	
Sex (M/F)	(49/18)	(73.2/26.8)	(28/14)	(66.7/33.3)	(12/8)	(60/40)
Surgery						
PPPD	59	88.1	39	92.9	18	90
Whipple–Kausch	8	11.9	3	7.1	2	10
Radicality						
R0 ( $\leq 1$ mm)	32	47.8	38	90.5	15	75
R1 ( $< 1$ mm)	27	40.3	4	9.5	5	25
Dubious	8	11.9	0	0	0	0
Diameter post-op (cm)						
1–2	1	1.5	N/A		N/A	
2–4	34	50.7	N/A		N/A	
4–6	17	25.4	N/A		N/A	
N/A	15	22.4				
N-stage						
N0	15	22.4	27	64.3	8	40
N1	52	77.6	15	35.7	12	60
Grading						
Well differentiated	2	3	N/A		N/A	
Moderately differentiated	18	26.9	N/A		N/A	
Poorly differentiated	21	31.3	N/A		N/A	
N/A	26	38.8				
Survival						
Median (range) (months)	18.33 (1.58–88.9)		49.92 (6.6–127.38)		24.36 (1.97–103.36)	

#### 4.3. Immunohistochemistry

C/EBP $\delta$  stainings were performed essentially as described before [54–57] with minor modifications. Four micron-thick paraffin embedded tissue sections were deparaffinized and treated with 0.3% H<sub>2</sub>O<sub>2</sub> in methanol for 15 min to block endogenous peroxidase activity. Subsequently, slides were blocked with Ultra V block (#TA-125-UB; Thermo Fisher Scientific, Waltham, MA, USA) and incubated with a rabbit polyclonal antibody against C/EBP $\delta$  (#GWB-MM818H; GenWay Biotech, San Diego, CA, USA) in a 1:1000 dilution in PBS at 4 °C overnight. The next day, slides were incubated with Powervision poly-HRP anti rabbit IgG (#DPVM-55HRP; Immunologic, Duiven, Netherlands) for 30 min at room temperature and stained using 3,3'-Diaminobenzidine (Bright DAB, #BS04-999; Immunologic). Hematoxylin (1:10 in demineralized H<sub>2</sub>O) was applied as counterstaining.

#### 4.4. Quantification of C/EBP $\delta$ Protein Levels

C/EBP $\delta$ -stained slides were reviewed by three independent pathologists in a blinded fashion to the clinical status of the patients. Specimens with conflicting scores were re-evaluated until consensus was reached. Nuclear C/EBP $\delta$  expression in tumor cells was scored based on the percentage of positively stained nuclei and the intensity of the positive staining. The percentage of positive nuclei for each core was scored on a scale from 0 to 3 (0: no positive nuclei, 1: less than 30% positive

nuclei, 2: between 30–70% positive nuclei, 3: more than 70% positive nuclei) whereas the intensity of the positive nuclei was scored on a scale from 1 to 3 (1: low intensity, 2: intermediate intensity, 3: high intensity). The intensity score (i.e., the average score of 10 randomly selected cells in three different areas of each core) was finally multiplied by the percentage score leading to a theoretical maximum score of 9. For survival analysis Kaplan–Meier curves were constructed using GraphPad Prism 6.0 (GraphPad Software Inc., La Jolla, CA, USA) whereby *C/EBPδ* expression levels were divided into an upper and a lower half based on the range observed in each type of tumor.

#### 4.5. Cell Lines and Cell Culture Reagents

Human PANC-1, MIA PaCa-2 and CAPAN-2 pancreatic cancer cell lines (ATCC, Manassas, VA, USA) were cultured in high glucose in Dulbecco's Modified Eagle Medium (Gibco, Thermo Fischer Scientific, Waltham, MA, USA) supplemented with 10% (*v/v*) fetal calf serum (FCS; Serana, Pessin, Germany), 2% (*v/v*) penicillin–streptomycin (Gibco, Thermo Fischer Scientific, Waltham, MA, USA) and 2 mM L-glutamine (Lonza, Basel, Switzerland). Cells were incubated in 5% CO<sub>2</sub> incubators at 37 °C. All cell lines were tested mycoplasma-negative and their identities have been confirmed by STR-profiling.

#### 4.6. RNA Isolation, cDNA Synthesis and RT-qPCR

To determine mRNA expression levels, RNA was extracted using the NucleoSpin<sup>®</sup> RNA-extraction Kit (Macherey-Nagel GmbH and Co. KG, Düren, Germany), according to the supplier's protocol for cultured cells. Eluted RNA was analyzed spectrophotometrically using the NanoDrop 2000. All samples were treated with RQ1 RNase-Free DNase (Promega Benelux BV, Leiden, Netherlands) and reverse-transcribed into cDNA using M-MLV Reverse Transcriptase (Promega Benelux BV, Leiden, Netherlands), random hexamers (Fisher scientific, Landsmeer, Netherlands) and 10 mM dNTPs (Fermentas, Fisher scientific, Landsmeer, Netherlands). The SensiFAST<sup>™</sup> SYBR<sup>®</sup> No-ROX Kit (GC biotech, Waddinxveen, Netherlands) was used to perform real-time quantitative RT-PCR on a LightCycler<sup>®</sup> 480 Instrument II (Roche Molecular Systems, Inc., Almere, Netherlands). *CEBPD* expression levels were normalized to the expression of the reference genes *TBP* and *GAPDH* or *TBP* (*EGFP* vs. *CEBPD*) using the following primers.

*GAPDH* forward primer (5'-3'): AAGGTGAAGGTCGGAGTCAAC;  
*GAPDH* reverse primer (5'-3'): TGGAAGATGGTGATGGGATT;  
*TBP* forward primer (5'-3'): ATCCCAAGCGGTTTGCTGC;  
*TBP* reverse primer (5'-3'): ACTGTTCTTCACTCTTGGCTC;  
*CEBPD* forward primer (5'-3'): GCAGAAGTTGGTGGAGCTGT;  
*CEBPD* reverse primer (5'-3'): TTACCGGCAGTCTGCTGTC;  
*EGFP* forward primer (5'-3'): AGCTGACCCTGAAGTTCATCTG;  
*EGFP* reverse primer (5'-3'): AAGTCGTGCTGCTTCATGTG;  
*CDK1* forward primer (5'-3'): CCCTTTAGCGCGGATCTA;  
*CDK1* reverse primer (5'-3'): ATGGCTACCACTTGACCTGT;  
*CDK2* forward primer (5'-3'): GAAAAGATCGGAGAGGGCA;  
*CDK2* reverse primer (5'-3'): ACCCTCAGTCTCAGTGTCCA;  
*CDK4* forward primer (5'-3'): TCTATGGTCGGGCCCTCTG;  
*CDK4* reverse primer (5'-3'): TCAGATCAAGGAGACCCT;  
*CDK6* forward primer (5'-3'): CTGCAGGGAAAGAAAAGTGC;  
*CDK6* reverse primer (5'-3'): TTCCCTCCTCGAAGCGAAG;  
*CDKN1A* forward primer (5'-3'): GCATGATCTGAGTTAGGTCAC;  
*CDKN1A* forward primer (5'-3'): GACATGGCGCCTGAACAGA;  
*BCL-2* forward primer (5'-3'): GGTGGGGTCATGTGTGTGG;  
*BCL-2* reverse primer (5'-3'): CGGTTCAGGTAAGTCAATCC;  
*BCL-XL* forward primer (5'-3'): AGAGAACAGGACTGAGGCCC;

BCL-XL reverse primer (5'-3'): TCAAAGCTCTGATATGCTGTCCC;  
 CD44 forward primer (5'-3'): AAGGTGGAGCAAACACAACC;  
 CD44 reverse primer (5'-3'): CTGAGACTTGCTGGCCTCTC;  
 TOP2A forward primer (5'-3'): TACATCCAAGGGTGGCAGAC;  
 TOP2A reverse primer (5'-3'): CCTGATGTGCTTTTACTGCAACA;  
 TTK forward primer (5'-3'): CATCAACATGGCATTGTTTAC;  
 TTK reverse primer (5'-3'): TCTGGTTGCATTTGGTTTGC;  
 ASPM forward primer (5'-3'): GTTGCAGACAAAGGCGGAAG;  
 ASPM reverse primer (5'-3'): CCTACTTCGTACATCAGAGGCTC;  
 ANLN forward primer (5'-3'): TTCCCAAAGGGATGGCGATG;  
 ANLN reverse primer (5'-3'): GGAGAAGTAGCTTTCACAGAGC;

#### 4.7. Gene Transfection and Transduction

PANC-1 cells were transfected with *pHEF-1TIG-CEBPD-IRES-EGFP* or *pHEF-1TIG-IRES-EGFP* using the Biontex K2 transfection system (Biontex, München, Germany) according to the supplier's protocol. For constitutive over-expression of C/EBP $\delta$ , a third-generation lentiviral system using *pHEF-1TIG-CEBPD-IRES-EGFP* or *pHEF-1TIG-IRES-EGFP*, *pMDLg/pRRE* (Addgene #12251), *pRSV-Rev* (Addgene # 12253) and *pMD2.G* (Addgene #12259) was employed to stably transduce PANC-1 and MIA-PaCa-2 cells. We have found that lentivirus production was enhanced in HEK293T cells expressing an shRNA targeting *CEBPD* (Figure S6B). Therefore, we used HEK293T cells stably transduced with an shRNA targeting *CEBPD* (MERCK MISSION<sup>®</sup> TRC-No, TRCN0000013969, clone ID NM\_005195.2-271s1c1) for all lentivirus productions. These producer cells were transfected for lentiviral production using Lipofectamine<sup>™</sup> 2000 Transfection Reagent (Figure S6A). The viral supernatant was collected 48 and 72 h after transfection, the virus was precipitated using PEG-it<sup>™</sup> Virus Precipitation Solution (System Bioscience, Cat No. LV810A-1) at 4 °C over the weekend and resuspended in 1/100 of the original volume. Then, 100  $\mu$ L was used to transduce 750,000 HEK293T cells in a 6-well plate by addition of the viral medium 24 h after seeding. For inducible over-expression of C/EBP $\delta$ , the *CEBPD* cDNA was cloned into the *pCW57* vector (Addgene # 80921) containing a doxycycline-controlled transactivator (tTA) that binds to the TRE promoter to initiate transcription of C/EBP $\delta$ . This vector was used with the same third-generation lentiviral system as above and prepared in the same way. Then, 25  $\mu$ L virus-containing medium was used to transduce 100,000 PANC-1 or MIA PaCa-2 cells in a 24-well plate. Forty-eight hours after transduction, cells were passaged and selected using 20 or 5  $\mu$ g/mL Blastocidin (Invitrogen # ant-bl-05). Single cells were seeded in 96-well plates and allowed to grow out. Per cell line, a pool of three clones with high inducibility and low leakiness of C/EBP $\delta$  expression was selected for subsequent experiments.

#### 4.8. Fluorescent Activated Cell Sorting

Forty-eight hours after transduction, the transduced cells were trypsinized and re-suspended in fluorescent activated cell sorting (FACS) buffer (PBS containing 1% FCS). The SONY SH800S Cell Sorter with single-cell sorting for clonogenic assays or two-way sorting to divide cells into EGFP-expression fractions was used. For MIA PaCa-2 cells, a 100  $\mu$ m sorting chip was used and for PANC-1 cells, a 130  $\mu$ m sorting chip was used. For RNA extraction, cells were sorted into RA1 lysis buffer (from NucleoSpin<sup>®</sup> RNA-extraction Kit, Ref. 740955, Macherey-Nagel GmbH and Co. KG, Düren, Germany) and further processed for RNA extraction and quantitative RT-PCR.

#### 4.9. Clonogenic Assay

Respective of the experiment, 100 cells were seeded into 24-well plates or 500 cells into a 12-well plate. Visible colonies were formed after two weeks. At this point, cells were fixed and stained using crystal violet (0.5% crystal violet in 30% ethanol/3% formaldehyde) for 10 min at room temperature followed by two washes in tap water. The colonies in 24-well plates were counted manually,

only including those that count at least 50 cells. Colonies in the 12-well plate were additionally counted and measured using countPHICS [58].

#### 4.10. Western Blot

Total protein was extracted by lysing cells in RIPA buffer (150 mM sodium chloride, 1% Triton X-100, 0.5% sodium deoxycholate, 0.1% SDS and 50 mM Tris (pH8.0)). Upon addition of Laemmli buffer (200 mM Tris-Cl (pH 6.8), 8% SDS, 0.4% Bromophenol blue and 40% glycerol) containing 2% 2-Mercaptoethanol, samples were fractionated by SDS/PAGE and transferred onto Immobilon-FL membranes (Millipore, Darmstadt, Germany). The blot was blocked in 5% BSA in PBS for 1 h at room temperature and incubated with primary antibodies against C/EBP $\delta$  (Santa Cruz Biotechnology, sc-365546, 1:500), eGFP (GeneTex, GTX26556, 1:5000) and  $\alpha$ -tubulin (Santa Cruz Biotechnology, sc-23948, 1:1000) in TBS with 0.1% Tween-20 over night at 4 °C. The blot was then washed in TBS with 0.1% Tween-20, incubated with secondary HRP-linked antibodies anti-rabbit-IgG (Cell Signaling, #7074, 1:1000) or anti-mouse-IgG (DAKO, P0447, 1:2500) for 1 h at room temperature in TBS with 0.1% Tween-20, washed again and incubated with ECL Western Blotting Substrate (Pierce, #32106, Thermo Fisher) for 10 min. The blot was imaged using the ImageQuant LAS 4000 (GE Healthcare Life Sciences, Eindhoven, Netherlands).

To visualize small differences of protein expression in doxycycline-induction experiments (Figure 5D,F), these Western blots were performed using the Wes™ Simple Western capillary-based automated immunoblotting system according to the standard protocol recommended by the supplier. The resulting images were processed using the Compass software for Simple Western (ProteinSimple, San Jose, CA, USA).

#### 4.11. Proliferation Assay

To assess the proliferative capacity of cell lines upon re-expression or knock-down of C/EBP $\delta$ , 10,000 cells (MIA PaCa-2 and PANC-1 transduced with a doxycycline-inducible over-expression plasmid or an empty control plasmid (*pCW57* plasmid, Addgene # 80921)) or 50,000 cells (Capan-2 transduced with shRNAs against C/EBP $\delta$  or tGFP) were seeded in 24-well plates in complete cell culture medium as described above or in the presence of 2000 ng/mL doxycycline (#D9891, Sigma-Aldrich N.V. Zwijndrecht, Netherlands) for 5 days (MIA PaCa-2 and PANC-1) and 8 days (Capan-2). Plates were scanned using the IncuCyte® S3 Live-Cell Analysis System (Sartorius, Göttingen, Germany). The confluence of experimental conditions was normalized to the respective control cell line.

#### 4.12. Soft Agar Tumor Sphere Formation Assay

From an autoclaved 5% agar (#30391-049, Thermo Fischer Scientific, Waltham, MA, USA) solution in saline, a 0.5% agar solution in Dulbecco's Modified Eagle Medium (Gibco, Thermo Fischer Scientific, Waltham, MA, USA) was prepared and 800  $\mu$ L was pipetted into 12-well plates to form a semi-solid bottom layer. From the same stock solution, three 0.3 % agar solutions were prepared in complete cell culture medium as described in Section 4.5 and supplemented with either no doxycycline, 100 ng/mL doxycycline or 2000 ng/mL doxycycline (#D9891, Sigma-Aldrich N.V. Zwijndrecht, Netherlands). Respectively, 6000 MIA PaCa-2 cells or 10,000 PANC-1 cells, each transduced with either a doxycycline-inducible C/EBP $\delta$  over-expression plasmid or an empty control plasmid (*pCW57* plasmid, Addgene # 80921) were added to 10 mL of 0.3% agar solution supplemented with or without doxycycline. Of the individual suspensions, 800  $\mu$ L was pipetted in triplicate onto the solidified 0.5% bottom layers and left to solidify. Wells were covered with complete cell culture medium supplemented with the respective concentration of doxycycline. Fresh medium was added twice per week without doxycycline or supplemented with 200 ng/mL or 4000 ng/mL doxycycline to ensure sufficient diffusion of doxycycline to the embedded cells. MIA PaCa-2 and PANC-1 cells were allowed to form tumor spheres for two and three weeks, respectively. All wells were then scanned using the EVOS® FL Cell Imaging System at 4 $\times$  magnification using bright field microscopy, to capture

all tumor spheres in a single plane. Spheres were then counted in Adobe Photoshop CS6 (Adobe® Photoshop® 2020 for Windows, San Jose, CA, USA) using the quick selection tool which was set to a diameter 23 px corresponding to 150 µm to count all spheres of this size and larger. The experiment was conducted 3 times.

#### 4.13. Knock-down of C/EBPδ in CAPAN-2 Cells

To knock down C/EBPδ in Capan-2 cells, a third-generation lentiviral system using pLKO.1 puro (#8453 Addgene) containing shRNAs against CEBPD or tGFP were used. Glycerol stocks were purchased from Sigma-Aldrich (St. Louis, MO, USA) (MISSION shRNA library). We selected clones TRCN0000013695 (shCEBPD #1), TRCN0000013696 (shCEBPD #2), TRCN0000013693 (shCEBPD #3) and TRCN0000013694 (shCEBPD #4) against CEBPD and SHC004 against turboGFP as control. Bacteria were seeded on agar plates containing 100 ng/mL ampicillin and single colonies were expanded in liquid cultures. Plasmids were purified (NucleoSpin® DNA, RNA and protein purification Kit, Ref. 740588.50, Macherey-Nagel GmbH and Co. KG, Düren, Germany) and incorporated in a 3rd generation lentivirus using *pMDLg/pRRE* (Addgene #12251), *pRSV-Rev* (Addgene # 12253) and *pMD2.G* (Addgene #12259). Lentiviruses were produced as described in Section 4.7 in normal HEK293T cells and Capan-2 cells were transduced in the same manner as described above and selected using Puromycin 1 µg/mL.

#### 4.14. Data Analysis

Statistical analyses were performed using GraphPad Prism 6.0 (GraphPad Software Inc., La Jolla, CA, USA). Using SPSS, the data were tested for significant outliers which were excluded from further analysis. Microarray data were analyzed using paired t-tests. Immunohistochemistry data and N-status were analyzed using the Mann–Whitney U test. Kaplan–Meier survival curves were analyzed using the Mantel–Cox log rank test. C/EBPδ-expression was correlated to lymph node involvement using a one-sided Fisher’s exact test. Survival data among CEBPD-low and CEBPD-high groups were compared using the Mann–Whitney U test. For in vitro experiments, data were analyzed using the Mann–Whitney U tests whereby a one-tailed *p*-value is given for the reduction in clonal outgrowth upon C/EBPδ over-expression. Pearson correlation was used to correlate CEBPD and EGFP expression, *p*-values are one-tailed. CEBPD mRNA values of Capan-2 knock-down cell lines were tested for normality using the Shapiro–Wilk test and two-tailed *p*-values were calculated using a parametric *t*-test. Two-way ANOVA with Greenhouse–Geisser correction was used to compare growth curves. Statistical significance was set at  $p < 0.05$ .

## 5. Conclusions

Pancreatic ductal adenocarcinoma is the most common and most fatal form of pancreatic cancer and, to date, only few tumor suppressor genes, including *TP53*, *SMAD4*, *PTEN* and *CDKN2A*, are formally established in this context [12,13]. Here, we have identified C/EBPδ as a novel putative tumor suppressor gene that is downregulated in pancreatic ductal adenocarcinoma but not in ampullary carcinoma or intrapancreatic cholangiocarcinoma. With this discovery, we add valuable insights to the biology of pancreatic cancer and the complex context-dependent role of C/EBPδ in tumorigenesis in general, and stress that this heterogeneity should be considered in clinical practice. Maybe more importantly, we have shown that re-expressing C/EBPδ limits pancreatic cancer cell growth in a dose-dependent manner, implying that re-expressing C/EBPδ in pancreatic ductal adenocarcinoma may limit disease progression, although this remains to be established in ongoing preclinical experimental animal studies.

**Supplementary Materials:** The following are available online at <http://www.mdpi.com/2072-6694/12/9/2546/s1>. Table S1: Fold change of leading edge genes from GSEAs between CEBPD-high and CEBPD-low groups, Table S2: Pearson correlation of CEBPD mRNA with stromal scores, Figure S1: CEBPD mRNA correlates with stromal scores in public datasets, Figure S2: Uncropped Western blot membrane corresponding to Figure 4C, Figure S3:

Uncropped Western blot membranes and WESTM Simple Western images, Figure S4: mRNA expression of CEBPD across PDAC cell lines, Figure S5: mRNA expression of putative targets of *CEBPD*, Figure S6: Establishment of lentivirus producer cells stably expressing *CEBPD*-shRNA.

**Author Contributions:** Conceptualization, L.H., J.D., M.F.B. and C.A.S.; data curation, F.D., G.K.J.H. and T.B.; formal analysis, L.H., J.D., P.Y.H., K.C., J.J.T.H.R., M.P.G.D., Q.P., M.P.P., M.F.B. and C.A.S.; funding acquisition, J.D.; investigation, L.H., J.D. and H.L.A.; methodology, L.H., J.D., M.F.B. and C.A.S.; project administration, J.D., M.F.B. and C.A.S.; resources, O.R.B., M.G.H.B., F.D., G.K.J.H. and T.B.; supervision, J.D., M.F.B. and C.A.S.; validation, L.H., J.D., P.Y.H., K.C. and J.J.T.H.R.; visualization, L.H., J.D., M.F.B. and C.A.S.; writing—original draft, L.H. and J.D.; writing—review and editing, L.H., J.D., O.R.B., M.G.H.B., F.D., G.K.J.H., P.Y.H., K.C., J.J.T.H.R., M.P.G.D., Q.P., M.P.P., M.F.B. and C.A.S. All authors have read and agreed to the published version of the manuscript.

**Funding:** This work was supported by a grant of the Dutch Cancer Foundation with number 2014-6782 and a VENI grant (J. Duitman 016.186.046) of the NWO. M.P.P. is grateful to the Dutch Society for the Replacement of Animal Testing and ZonMw (2016/22827/ZONMW) for their financial support. The funders have not participated in the study design, data collection, data analysis, interpretation, or writing of the report.

**Acknowledgments:** The authors would like to thank Onno de Boer for his help with the digitalization of the stainings. The results shown here are in whole or part based upon data generated by the TCGA Research Network: <https://www.cancer.gov/tcga>.

**Conflicts of Interest:** M.F.B. has received research funding from Servier and has acted as a consultant for Celgene. Neither was involved in the design of this study or drafting of the manuscript. All authors declare no conflict of interest.

## References

- Jemal, A.; Bray, F.; Center, M.M.; Ferlay, J.; Ward, E.; Forman, D. Global cancer statistics. *CA Cancer J. Clin.* **2011**, *61*, 69–90. [[CrossRef](#)]
- Stark, A.P.; Sacks, G.D.; Rochefort, M.M.; Donahue, T.R.; Reber, H.A.; Tomlinson, J.S.; Dawson, D.W.; Eibl, G.; Hines, O.J. Long-term Survival in Patients with Pancreatic Ductal Adenocarcinoma. *Surgery* **2016**, *159*, 1520–1527. [[CrossRef](#)]
- Yao, W.; Maitra, A.; Ying, H. Recent insights into the biology of pancreatic cancer. *EBioMedicine* **2020**, *53*, e102655. [[CrossRef](#)]
- Hidalgo, M. Pancreatic cancer. *N. Engl. J. Med.* **2010**, *362*, 1605–1617. [[CrossRef](#)]
- Ryan, D.P.; Hong, T.S.; Bardeesy, N. Pancreatic adenocarcinoma. *N. Engl. J. Med.* **2014**, *371*, 1039–1049. [[CrossRef](#)]
- Christenson, E.S.; Jaffee, E.; Azad, N.S. Current and emerging therapies for patients with advanced pancreatic ductal adenocarcinoma: A bright future. *Lancet Oncol.* **2020**, *21*, e135–e145. [[CrossRef](#)]
- Cardenes, H.R.; Chiorean, E.G.; Dewitt, J.; Schmidt, M.; Loehrer, P. Locally advanced pancreatic cancer: Current therapeutic approach. *Oncologist* **2006**, *11*, 612–623. [[CrossRef](#)]
- Gharibi, A.; Adamian, Y.; Kelber, J.A. Cellular and molecular aspects of pancreatic cancer. *Acta. Histochem.* **2016**, *118*, 305–316. [[CrossRef](#)]
- Ahn, D.H.; Bekaii-Saab, T. Ampullary cancer: An overview. *Am. Soc. Clin. Oncol. Educ. Book* **2014**, *34*, 112–115. [[CrossRef](#)]
- Freeny, P.C. Computed tomography in the diagnosis and staging of cholangiocarcinoma and pancreatic carcinoma. *Ann. Oncol.* **1999**, *10*, 12–17. [[CrossRef](#)]
- Hrad, V.; Abebe, Y.; Ali, S.H.; Velgersdyk, J.; Al Hallak, M.; Imam, M. Risk and Surveillance of Cancers in Primary Biliary Tract Disease. *Gastroenterol. Res. Pract.* **2016**, *2016*, e3432640. [[CrossRef](#)]
- Cicenas, J.; Kvederaviciute, K.; Meskinyte, I.; Meskinyte-Kausiliene, E.; Skeberdyte, A. KRAS, TP53, CDKN2A, SMAD4, BRCA1, and BRCA2 Mutations in Pancreatic Cancer. *Cancers* **2017**, *9*, e42. [[CrossRef](#)] [[PubMed](#)]
- Ying, H.; Elpek, K.G.; Vinjamoori, A.; Zimmerman, S.M.; Chu, G.C.; Yan, H.; Fletcher-Sananikone, E.; Zhang, H.; Liu, Y.; Wang, W.; et al. PTEN is a major tumor suppressor in pancreatic ductal adenocarcinoma and regulates an NF- $\kappa$ B-cytokine network. *Cancer Discov.* **2011**, *1*, 158–169. [[CrossRef](#)] [[PubMed](#)]
- Ramji, D.P.; Foka, P. CCAAT/enhancer-binding proteins: Structure, function and regulation. *Biochem. J.* **2002**, *365*, 561–575. [[CrossRef](#)]
- Sivko, G.S.; DeWille, J.W. CCAAT/enhancer binding protein delta (C/EBP delta) regulation and expression in human mammary epithelial cells: I. “Loss of function” alterations in the C/EBP delta growth inhibitory pathway in breast cancer cell lines. *J. Cell. Biochem.* **2004**, *93*, 830–843. [[CrossRef](#)] [[PubMed](#)]

16. Pawar, S.A.; Sarkar, T.R.; Balamurugan, K.; Sharan, S.; Wang, J.; Zhang, Y.; Dowdy, S.F.; Huang, A.M.; Sterneck, E. C/EBPdelta targets cyclin D1 for proteasome-mediated degradation via induction of CDC27/APC3 expression. *Proc. Natl. Acad. Sci. USA* **2010**, *107*, 9210–9215. [[CrossRef](#)]
17. Gery, S.; Tanosaki, S.; Hofmann, W.K.; Koppel, A.; Koeffler, H.P. C/EBPdelta expression in a BCR-ABL-positive cell line induces growth arrest and myeloid differentiation. *Oncogene* **2005**, *24*, 1589–1597. [[CrossRef](#)]
18. Pan, Y.C.; Li, C.F.; Ko, C.Y.; Pan, M.H.; Chen, P.J.; Tseng, J.T.; Wu, W.C.; Chang, W.C.; Huang, A.M.; Sterneck, E.; et al. CEBPD reverses RB/E2F1-mediated gene repression and participates in HMDB-induced apoptosis of cancer cells. *Clin. Cancer Res.* **2010**, *16*, 5770–5780. [[CrossRef](#)]
19. O'Rourke, J.; Yuan, R.; DeWille, J. CCAAT/enhancer-binding protein-delta (C/EBP-delta) is induced in growth-arrested mouse mammary epithelial cells. *J. Biol. Chem.* **1997**, *272*, 6291–6296. [[CrossRef](#)]
20. Thangaraju, M.; Rudelius, M.; Bierie, B.; Raffeld, M.; Sharan, S.; Hennighausen, L.; Huang, A.M.; Sterneck, E. C/EBPdelta is a crucial regulator of pro-apoptotic gene expression during mammary gland involution. *Development* **2005**, *132*, 4675–4685. [[CrossRef](#)]
21. Mendoza-Villanueva, D.; Balamurugan, K.; Ali, H.R.; Kim, S.R.; Sharan, S.; Johnson, R.C.; Merchant, A.S.; Caldas, C.; Landberg, G.; Sterneck, E. The C/EBP $\delta$  protein is stabilized by estrogen receptor  $\alpha$  activity, inhibits SNAIL2 expression and associates with good prognosis in breast cancer. *Oncogene* **2016**, *35*, 6166–6176. [[CrossRef](#)] [[PubMed](#)]
22. Palmieri, C.; Monteverde, M.; Lattanzio, L.; Gojis, O.; Rudraraju, B.; Fortunato, M.; Syed, N.; Thompson, A.; Garrone, O.; Merlano, M.; et al. Site-specific CpG methylation in the CCAAT/enhancer binding protein delta (CEBP $\delta$ ) CpG island in breast cancer is associated with metastatic relapse. *Br. J. Cancer* **2012**, *107*, 732–738. [[CrossRef](#)] [[PubMed](#)]
23. Tang, D.; Sivko, G.S.; DeWille, J.W. Promoter methylation reduces C/EBPdelta (CEBPD) gene expression in the SUM-52PE human breast cancer cell line and in primary breast tumors. *Breast Cancer Res. Treat.* **2006**, *95*, 161–170. [[CrossRef](#)] [[PubMed](#)]
24. Sowamber, R.; Chehade, R.; Bitar, M.; Dodds, L.V.; Milea, A.; Slomovitz, B.; Shaw, P.A.; George, S.H.L. CCAAT/enhancer binding protein delta (C/EBP $\delta$ ) demonstrates a dichotomous role in tumor initiation and promotion of epithelial carcinoma. *EBioMedicine* **2019**, *44*, 261–274. [[CrossRef](#)] [[PubMed](#)]
25. Ko, C.Y.; Hsu, H.C.; Shen, M.R.; Chang, W.C.; Wang, J.M. Epigenetic silencing of CCAAT/enhancer-binding protein delta activity by YY1/polycomb group/DNA methyltransferase complex. *J. Biol. Chem.* **2008**, *283*, 30919–33032. [[CrossRef](#)]
26. Agrawal, S.; Hofmann, W.K.; Tidow, N.; Ehrich, M.; Van den Boom, D.; Koschmieder, S.; Berdel, W.E.; Serve, H.; Müller-Tidow, C. The C/EBPdelta tumor suppressor is silenced by hypermethylation in acute myeloid leukemia. *Blood* **2007**, *109*, 3895–3905. [[CrossRef](#)]
27. Li, C.F.; Tsai, H.H.; Ko, C.Y.; Pan, Y.C.; Yen, C.J.; Lai, H.Y.; Yuh, C.H.; Wu, W.C.; Wang, J.M. HMDB and 5-AzadC Combination Reverses Tumor Suppressor CCAAT/Enhancer-Binding Protein Delta to Strengthen the Death of Liver Cancer Cells. *Mol. Cancer Ther.* **2015**, *14*, 2623–2633. [[CrossRef](#)]
28. Liu, P.; Cao, W.; Ma, B.; Li, M.; Chen, K.; Sideras, K.; Duitman, J.W.; Sprengers, D.; Khe Tran, T.C.; Ijzermans, J.N.M.; et al. Action and clinical significance of CCAAT/enhancer-binding protein delta in hepatocellular carcinoma. *Carcinogenesis* **2019**, *40*, 155–163. [[CrossRef](#)]
29. Cooper, L.A.; Gutman, D.A.; Chisolm, C.; Appin, C.; Kong, J.; Rong, Y.; Kurc, T.; Van Meir, E.G.; Saltz, J.H.; Moreno, C.S.; et al. The tumor microenvironment strongly impacts master transcriptional regulators and gene expression class of glioblastoma. *Am. J. Pathol.* **2012**, *180*, 2108–2119. [[CrossRef](#)]
30. Balamurugan, K.; Wang, J.; Tsai, H.; Sharan, S.; Anver, A.; Leighty, R.; Sterneck, E. The tumour suppressor C/EBP $\delta$  inhibits FBXW7 expression and promotes mammary tumour metastasis. *EMBO J.* **2010**, *29*, 4106–4117. [[CrossRef](#)]
31. Wang, Y.H.; Wu, W.J.; Wang, W.J.; Huang, H.Y.; Li, W.M.; Yeh, B.W.; Wu, T.F.; Shiue, Y.L.; Sheu, J.J.; Wang, J.M.; et al. CEBPD amplification and overexpression in urothelial carcinoma: A driver of tumor metastasis indicating adverse prognosis. *Oncotarget* **2015**, *6*, 31069–31084. [[CrossRef](#)] [[PubMed](#)]
32. Wu, S.R.; Li, C.F.; Hung, L.Y.; Huang, A.M.; Tseng, J.T.; Tsou, J.H.; Wang, J.M. CCAAT/enhancer-binding protein delta mediates tumor necrosis factor alpha-induced Aurora kinase C transcription and promotes genomic instability. *J. Biol. Chem.* **2011**, *286*, 28662–28670. [[CrossRef](#)] [[PubMed](#)]

33. Zhang, G.; Schetter, A.; He, P.; Funamizu, N.; Gaedcke, J.; Ghadimi, B.M.; Ried, T.; Hassan, R.; Yfantis, H.G.; Lee, D.H.; et al. DPEP1 inhibits tumor cell invasiveness, enhances chemosensitivity and predicts clinical outcome in pancreatic ductal adenocarcinoma. *PLoS ONE* **2012**, *7*, e31507. [CrossRef]
34. Pei, H.; Li, L.; Fridley, B.L.; Jenkins, G.D.; Kalari, K.R.; Lingle, W.; Petersen, G.; Lou, Z.; Wang, L. FKBP51 affects cancer cell response to chemotherapy by negatively regulating Akt. *Cancer Cell*. **2009**, *16*, 259–266. [CrossRef] [PubMed]
35. Ben-Porath, I.; Thomson, M.W.; Carey, V.J.; Ge, R.; Bell, G.W.; Regev, A.; Weinberg, R.A. An embryonic stem cell-like gene expression signature in poorly differentiated aggressive human tumors. *Nat. Genet.* **2008**, *40*, 499–507. [CrossRef]
36. Chiang, D.Y.; Villanueva, A.; Hoshida, Y.; Peix, J.; Nevell, P.; Minguez, B.; LeBlanc, A.C.; Donovan, D.J.; Thung, S.N.; Sole, M.; et al. Focal Gains of Vascular Endothelial Growth Factor A and Molecular Classification of Hepatocellular Carcinoma. *Cancer Res.* **2008**, *68*, 6779–6788. [CrossRef]
37. Chen, Y.; Chen, F.; Chang, T.; Wang, T.; Hsu, T.; Chi, J.; Hsiao, Y.; Li, C.; Wang, J. Hepatoma-derived growth factor supports the antiapoptosis and profibrosis of pancreatic stellate cells. *Cancer Lett.* **2019**, *457*, 180–190. [CrossRef]
38. Badea, L.; Herlea, V.; Dima, S.O.; Dumitrascu, T.; Popescu, I. Combined gene expression analysis of whole-tissue and microdissected pancreatic ductal adenocarcinoma identifies genes specifically overexpressed in tumor epithelia. *Hepato Gastroenterol.* **2008**, *55*, 2016–2027.
39. Grimont, A.; Pinho, A.V.; Cowley, M.J.; Augereau, C.; Mawson, A.; Giry-Laterriere, M.; Van den Steen, G.; Waddell, N.; Pajic, M.; Sempoux, C.; et al. SOX9 regulates ERBB signalling in pancreatic cancer development. *Gut* **2015**, *64*, 1790–1799. [CrossRef]
40. Raphael, B.J.; Aguirre, A.J. Cancer Genome Atlas Research Network. Integrated Genomic Characterization of Pancreatic Ductal Adenocarcinoma. *Cancer Cell*. **2017**, *32*, 185–203. [CrossRef]
41. Yang, S.; He, P.; Wang, J.; Schetter, A.; Tang, W.; Funamizu, N.; Yanaga, K.; Uwagawa, T.; Satoskar, A.R.; Gaedcke, J.; et al. A Novel MIF Signaling Pathway Drives the Malignant Character of Pancreatic Cancer by Targeting NR3C2. *Cancer Res.* **2016**, *76*, 3838–3850. [CrossRef] [PubMed]
42. Dijk, F.; Veenstra, V.L.; Soer, E.C.; Dings, M.P.G.; Zhao, L.; Halfwerk, J.B.; Hooijer, G.K.; Damhofer, H.; Marzano, M.; Steins, A.; et al. Unsupervised class discovery in pancreatic ductal adenocarcinoma reveals cell-intrinsic mesenchymal features and high concordance between existing classification systems. *Sci. Rep.* **2020**, *10*, e337. [CrossRef]
43. Yoshihara, K.; Shahmoradian, M.; Martinez, E.; Vegesna, R.; Hoon, K.; Torres-Garcia, W.; Trevino, V.; Shen, H.; Laird, P.W.; Levine, D.A.; et al. Inferring tumour purity and stromal and immune cell admixture from expression data. *Nat. Commun.* **2013**, *4*, e2612. [CrossRef] [PubMed]
44. Mori, S.; Chang, J.T.; Andrechek, E.R.; Matsumura, N.; Baba, T.; Yao, G.; Kim, J.W.; Gatzka, M.; Murphy, S.; Nevins, J.R. Anchorage-independent cell growth signature identifies tumors with metastatic potential. *Oncogene* **2009**, *28*, 2790–2805. [CrossRef] [PubMed]
45. Maupin, K.A.; Sinha, A.; Eugster, E.; Miller, J.; Ross, J.; Paulino, V.; Keshamouni, V.G.; Tran, N.; Berens, M.; Webb, C.; et al. Glycogene expression alterations associated with pancreatic cancer epithelial-mesenchymal transition in complementary model systems. *PLoS ONE* **2010**, *5*, e13002. [CrossRef] [PubMed]
46. R2: Genomics Analysis and Visualization Platform. Available online: <http://r2.amc.nl> (accessed on 5 August 2020).
47. Balamurugan, K.; Sterneck, E. The many faces of C/EBP $\delta$  and their relevance for inflammation and cancer. *Int. J. Biol. Sci.* **2013**, *9*, 917–933. [CrossRef]
48. Cerami, E.; Gao, J.; Dogrusoz, U.; Gross, B.E.; Sumer, S.O.; Aksoy, B.A.; Jacobsen, A.; Byrne, C.J.; Heuer, M.L.; Larsson, E.; et al. The cBio Cancer Genomics Portal: An Open Platform for Exploring Multidimensional Cancer Genomics Data. *Cancer Dis.* **2012**, *2*, 401–404. [CrossRef]
49. Gao, J.; Aksoy, B.A.; Dogrusoz, U.; Dresdner, G.; Gross, B.; Sumer, S.O.; Sun, Y.; Jacobsen, A.; Sinha, R.; Larsson, E.; et al. Integrative analysis of complex cancer genomics and clinical profiles using the cBioPortal. *Sci. Signal.* **2013**, *6*, 269. [CrossRef]
50. Broad Institute; Firehose Broad GDAC; PAAD. Available online: <https://gdac.broadinstitute.org/> (accessed on 3 December 2019).
51. DeWille, J.W.; Sanford, D.C. C/EBP $\delta$  is a downstream mediator of IL-6 induced growth inhibition of prostate cancer cells. *Prostate* **2005**, *63*, 143–154. [CrossRef]

52. Tsai, H.H.; Lai, H.Y.; Chen, Y.C.; Li, C.F.; Huang, H.S.; Liu, H.S.; Tsai, Y.S.; Wang, J.M. Metformin promotes apoptosis in hepatocellular carcinoma through the CEBPD-induced autophagy pathway. *Oncotarget* **2017**, *8*, 13832–13845. [[CrossRef](#)]
53. Ko, C.Y.; Chang, W.C.; Wang, J.M. Biological roles of CCAAT/Enhancer-binding protein delta during inflammation. *J. Biomed. Sci.* **2015**, *22*, e6. [[CrossRef](#)] [[PubMed](#)]
54. Valls Serón, M.; Duitman, J.; Geldhoff, M.; Engelen-Lee, J.; Havik, S.R.; Brouwer, M.C.; Van de Beek, D.; Spek, C.A. CCAAT/enhancer-binding protein  $\delta$  (C/EBP $\delta$ ) aggravates inflammation and bacterial dissemination during pneumococcal meningitis. *J. Neuroinflamm.* **2015**, *12*, e88. [[CrossRef](#)] [[PubMed](#)]
55. Duitman, J.; Schouten, M.; Groot, A.P.; Daalhuisen, J.B.; Florquin, S.; Van der Poll, T.; Spek, C.A. CCAAT/enhancer-binding protein  $\delta$  facilitates bacterial dissemination during pneumococcal pneumonia in a platelet-activating factor receptor-dependent manner. *Proc. Natl. Acad. Sci. USA* **2012**, *109*, 9113–9118. [[CrossRef](#)] [[PubMed](#)]
56. Duitman, J.; Hoogendijk, A.J.; Groot, A.P.; Ruela, R.R.; Van der Poll, T.; Florquin, S.; Spek, C.A. CCAAT-Enhancer-Binding Protein delta (C/EBP $\delta$ ) protects against Klebsiella-pneumoniae-induced pulmonary infection; potential role for macrophage migration. *J. Infect. Dis.* **2012**, *206*, 1826–1835. [[CrossRef](#)] [[PubMed](#)]
57. Duitmann, J.; Cong, L.; Moog, S.; Jaillet, M.; Castier, Y.; Cazes, A.; Borensztajn, K.S.; Crestani, B.; Speck, C.A. CCAAT/enhancer binding protein delta (C/EBP $\delta$ ) deficiency does not affect bleomycin-induced pulmonary fibrosis. *J. Transl. Res.* **2018**, *3*, 358–365. [[CrossRef](#)]
58. Brzozowska, B.; Galecki, M.; Tartas, A.; Ginter, J.; Kazmierczak, U.; Lundholm, L. Freeware tool for analysing numbers and sizes of cell colonies. *Radiat. Environ. Biophys.* **2019**, *58*, e109. [[CrossRef](#)]



© 2020 by the authors. Licensee MDPI, Basel, Switzerland. This article is an open access article distributed under the terms and conditions of the Creative Commons Attribution (CC BY) license (<http://creativecommons.org/licenses/by/4.0/>).